

Isolation and Molecular Structure of a Monomeric, Tris[peroxotitanium(IV)]-Substituted α -Dawson Polyoxometalate Derived from the Tetrameric Anhydride Form Composed of Four Tris[titanium(IV)]-Substituted α -Dawson Substructures and Four Bridging Titanium(IV) Octahedral Groups

Yoshitaka Sakai,^[a] Yuh Kitakoga,^[a] Kunihiro Hayashi,^[a] Kenji Yoza,^[b] and Kenji Nomiya^{*[a]}

Keywords: Titanium(IV) / Peroxo complexes / Polyoxometalates

The isolation and structural characterisation of a novel tris[peroxotitanium(IV)]-substituted α -Dawson polyoxometalate (POM), $[\alpha\text{-}1,2,3\text{-P}_2\text{W}_{15}(\text{TiO}_2)_3\text{O}_{56}(\text{OH})_3]^{9-}$ (**1a**), containing side-on coordination (i.e. η^2 -coordination) of the peroxo group to the titanium(IV) atom are described. A water-soluble, completely inorganic compound of the monomeric POM $\text{Na}_9[\alpha\text{-}1,2,3\text{-P}_2\text{W}_{15}(\text{TiO}_2)_3\text{O}_{56}(\text{OH})_3]\cdot 16\text{H}_2\text{O}$ (**1**), obtained as analytically pure, homogeneous orange crystals, was obtained from a reaction in aqueous solution of an excess of 30% aqueous hydrogen peroxide with $\{[\alpha\text{-}1,2,3\text{-P}_2\text{W}_{15}\text{Ti}_3\text{O}_{59}(\text{OH})_3]_4[\mu_3\text{-Ti}(\text{OH})_3]_4\text{Cl}\}^{33-}$ (**2a**). The latter has been recently shown to be a giant "tetrapod"-shaped, tetrameric anhydride formed from the tris[titanium(IV)]-substituted Dawson substructures with four bridging Ti octahedral

groups. Compound **1** could not be obtained from the reaction with another giant tetrapod POM, $\{[\alpha\text{-}1,2,3\text{-P}_2\text{W}_{15}\text{Ti}_3\text{O}_{57.5}(\text{OH})_3]_4\text{Cl}\}^{25-}$ (**3a**), which does not contain the bridging octahedral Ti groups. The molecular structure of **1a** was successfully determined by a single-crystal X-ray diffraction study and was shown to be a monomeric α -Dawson POM derived from the tris[peroxotitanium(IV)] species. Bond valence sum (BVS) calculations suggest that the μ_2 -oxo sites of the three Ti–O–Ti bridges in the Ti_3 cap of the Dawson unit are protonated. Characterisation of **1** was also accomplished by complete elemental analysis, TG/DTA, FTIR and solution (^{31}P and ^{183}W) NMR spectroscopy. (© Wiley-VCH Verlag GmbH & Co. KGaA, 69451 Weinheim, Germany, 2004)

Introduction

Polyoxometalates (POMs) are molecular metal oxide clusters. They are of current interest as soluble metal oxides and because of their applications in catalysis, medicine and materials science.^[1] Site-selective substitution of the W^{VI} atoms in POMs with Ti^{IV} atoms is particularly interesting because of the multicentre active sites formed with corner- and/or edge-sharing TiO_6 octahedra and the water-soluble molecular modelling studies of titanium(IV) oxides as an effective semiconductor and photocatalysts.^[2]

Many H_2O_2 -based oxidation reactions catalysed by titanium(IV)-substituted POMs have been described in which the peroxotitanium(IV) and/or hydroperoxotitanium(IV) species have been proposed as the active intermediates in such reactions.^[3] Thus, the synthesis and structural characterisation of peroxotitanium(IV)-substituted POMs would

constitute an intriguing project. Only a few structure determinations of peroxotitanium(IV) complexes have been conducted and these have been for the mono[peroxotitanium(IV)]-substituted Keggin POM $[\text{PW}_{11}(\text{TiO}_2)\text{O}_{39}]^{5-}$ species,^[4] whereas related examples from the Dawson POM family have not been reported so far.

Very recently, we reported the two tetrameric anhydride forms of tri- Ti^{IV} -substituted Dawson POMs, i.e. $\{[\alpha\text{-}1,2,3\text{-P}_2\text{W}_{15}\text{Ti}_3\text{O}_{59}(\text{OH})_3]_4[\mu_3\text{-Ti}(\text{OH})_3]_4\text{Cl}\}^{33-}$ (**2a**, tetrapod-shaped POM with the four bridging octahedral Ti^{IV} groups and with one encapsulated Cl^- ion)^[5a] and $\{[\alpha\text{-}1,2,3\text{-P}_2\text{W}_{15}\text{Ti}_3\text{O}_{57.5}(\text{OH})_3]_4\text{Cl}\}^{25-}$ (**3a**, tetrapod-shaped POM without the bridging octahedral Ti^{IV} groups and with one encapsulated Cl^- ion),^[5b] both of which contain a giant, inorganic "tetrapod" molecule composed of four 1,2,3-tri- Ti^{IV} -substituted α -Dawson substructures.^[6,7] Separately, Kortz et al. have also determined the molecular structure of the related tetrameric Dawson species without encapsulated chloride ions, $\{[\text{P}_2\text{W}_{15}\text{Ti}_3\text{O}_{57.5}(\text{OH})_3]_4\}^{24-}$ (**4a**).^[5c,6,7]

During our study of the formation of **2a** and **3a** in aqueous solution^[8] and the reactivity of these species with hydrogen peroxide (see the Exp. Sect.), we unexpectedly obtained a monomeric and pure form of the tris[peroxotitanium(IV)]-substituted Dawson POM $[\alpha\text{-}1,2,3\text{-}$

^[a] Kanagawa University, Tsuchiya 2946, Hiratsuka, Kanagawa 259-1293, Japan
Fax: (internat.) + 81-463-58-9684
E-mail: nomiya@chem.kanagawa-u.ac.jp

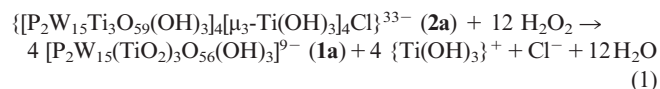
^[b] Nihon Bruker AXS, Kanagawa-ku, Moriyacho 3-9 A6F, Yokohama 221-0022, Japan
Supporting information for this article is available on the WWW under <http://www.eurjic.org> or from the author.

$\text{P}_2\text{W}_{15}(\text{TiO}_2)_3\text{O}_{56}(\text{OH})_3]^{9-}$ (**1a**) from the reaction of **2a**. The reaction of **3a**, however, did not produce such a result. An X-ray structure analysis revealed that the peroxo groups on the Ti atoms are attached by side-on coordination, i.e. η^2 -coordination. The bond valence sum (BVS) calculations of the oxygen atoms suggest that three protons are bound to the surface edge-sharing oxygen atoms of the Ti_3 cap in **1a**. The lack of any other protons in **1a** conclusively suggests that the peroxo group, but not the hydroperoxo group, is bound to the Ti atom. The X-ray structure determination of the POM-based tris[peroxotitanium(IV)] complex highlighted here is the first example of its type. Herein, we report full details of the synthesis and characterisation of the water-soluble sodium salt $\text{Na}_9[\text{1a}] \cdot 16\text{H}_2\text{O}$ (**1**) and the molecular structure of **1a**.

Results and Discussion

Synthesis, Isolation and Characterisation of **1**

The water-soluble sodium salt of **1** was prepared in ca. 25% (0.53 g scale) yield by recrystallising the orange powder which was obtained from the reaction of the precursor **2** in aqueous solution with an excess of 30% aqueous H_2O_2 . Of particular note is the fact that the reactivity of the two tetrameric Dawson POMs **2** and **3** with aqueous hydrogen peroxide was remarkably different. Compound **1** was successfully derived from the reaction of **2** with aqueous H_2O_2 , but **3** did not behave in such a way. The formation of **1a** is shown in Equation (1).



Compound **1** was characterised by complete elemental analysis, TG/DTA, FTIR, ^{31}P and ^{183}W NMR spectroscopy and a single-crystal X-ray diffraction study. The sample for elemental analysis was prepared by drying at room temperature under a vacuum of 10^{-3} – 10^{-4} Torr overnight. All elements were observed, including oxygen, to a total analysis of 98.95 %. These data are consistent with a composition of $\text{Na}_9[\text{1a}] \cdot 4\text{H}_2\text{O}$. The weight loss observed during the course of drying before analysis was 4.93% which corresponded to 12–13 water molecules weakly bound or adsorbed in **1**. In contrast, TG/DTA measurements performed under atmospheric conditions showed a weight loss of 6.61% between 25 and 168 °C with endothermic points at 60 and 84 °C corresponding to the presence of 16 water molecules constituting both the intrinsic water of hydration and adsorbed water from the atmosphere. The number of water molecules (16) is consistent with the sum of the water molecules (4) found in the elemental analysis plus the water molecules (12–13) corresponding to the weight loss observed during the course of drying before analysis. Interestingly, bond-valence sum (BVS) calculations of the oxygen atoms in **1a** indicate that

the μ_2 -oxo sites of the three Ti–O–Ti bridges in the Dawson unit are protonated (see “Molecular Structure of **1a**”).

TG/DTA measurements also showed the thermal stability of **1**. A weight loss of 4.12% observed from 167 °C up to ca. 400 °C with an endothermic point at 172 °C was due to decomposition of the coordinated peroxo groups. FTIR spectroscopic measurements of the samples after heating up to 150 °C (resulting in dehydration) and 200 °C (resulting in decomposition of the peroxo groups) showed that the Dawson POM framework was still intact. However, the IR measurements of the sample after heating up to 500 °C showed that the Dawson framework had been disrupted.

The solid-state FTIR spectrum of **1** (Figure 1, a; $\tilde{\nu} = 1083, 940, 923, 800 \text{ br cm}^{-1}$) measured as a KBr disk, showed the characteristic vibrational bands of the Dawson-type POM “ $\text{P}_2\text{W}_{18}\text{O}_{62}^{6-}$ ” framework.^[9] The lack of bands at around 650 cm^{-1} which would be due to an inter-Dawson unit Ti–O–Ti vibration suggests that **1** is a monomer and not an oligomer. The O–O stretching band which is known to appear around 900 cm^{-1} for monoperoxo complexes^[10] was observed at 890 cm^{-1} .

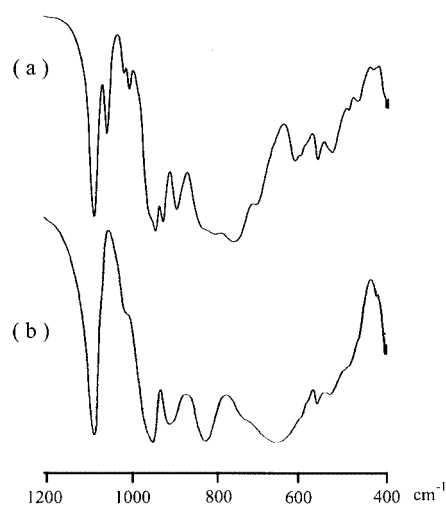


Figure 1. FTIR spectra in the polyoxoanion region (1200–400 cm^{-1}), measured as KBr disks, of a) $\text{Na}_9[\text{1a}] \cdot 16\text{H}_2\text{O}$ (**1**) [$\text{1a} = [\alpha\text{-}1,2,3\text{-P}_2\text{W}_{15}(\text{TiO}_2)_3\text{O}_{56}(\text{OH})_3]^{9-}$] and b) $\text{Na}_x\text{H}_{33-x}[\text{2a}] \cdot y\text{H}_2\text{O}$ (**2**) ($x = 16\text{--}19$, $y = 60\text{--}70$; **2a** = $\{[\alpha\text{-}1,2,3\text{-P}_2\text{W}_{15}\text{Ti}_3\text{O}_{59}(\text{OH})_3]_4[\mu_3\text{-Ti}(\text{OH})_3\text{Cl}]^{33-}\}$)

The ^{183}W NMR spectrum of **1** measured in D_2O at 20.7 °C (Figure 2, a) showed a three-line pattern with signals at $\delta = -156.5, -201.9$ and -230.1 ppm with relative intensities of 1:2:2. This spectrum is in agreement with the presence of two tungsten belts consisting of six WO_6 octahedra and a tungsten cap of three WO_6 octahedra. The ^{31}P NMR spectrum of **1** in D_2O at 22.6 °C (Figure 3, a) showed a clean two-line pattern with signals at $\delta = -3.93$ and -14.41 ppm, confirming its purity and single-product nature. The downfield resonance can be assigned to the phosphorus atom closest to the Ti_3 cap, whereas the upfield resonance is due to the phosphorus atom closer to the W_3 cap. It should be noted that the downfield signal is much more shifted to low-field compared with those of the tetrameric

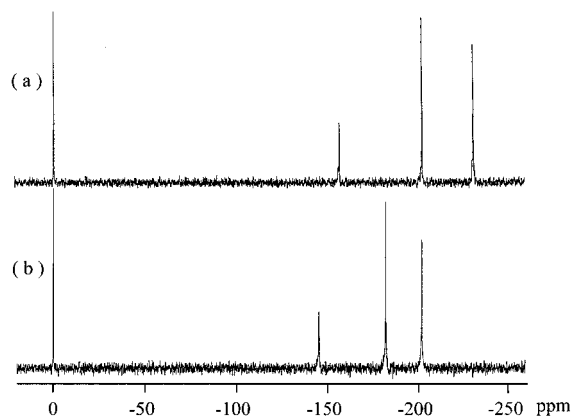


Figure 2. ^{183}W NMR spectra in D_2O of a) $\text{Na}_9[\mathbf{1a}] \cdot 16\text{H}_2\text{O}$ ($\mathbf{1}$) $\{\alpha\text{-}1,2,3\text{-P}_2\text{W}_{15}(\text{TiO}_2)_3\text{O}_{56}(\text{OH})_3\}^{9-}$ and b) $\text{Na}_x\text{H}_{33-x}[\mathbf{2a}] \cdot y\text{H}_2\text{O}$ ($\mathbf{2}$) ($x = 16\text{--}19$, $y = 60\text{--}70$; $\mathbf{2a} = \{\alpha\text{-}1,2,3\text{-P}_2\text{W}_{15}\text{Ti}_3\text{O}_{59}(\text{OH})_3\}_4[\mu_3\text{-Ti}(\text{OH})_3\text{Cl}]^{33-}$); the resonance at $\delta = 0.0$ ppm is due to the external reference saturated $\text{Na}_2\text{WO}_4/\text{D}_2\text{O}$ solution

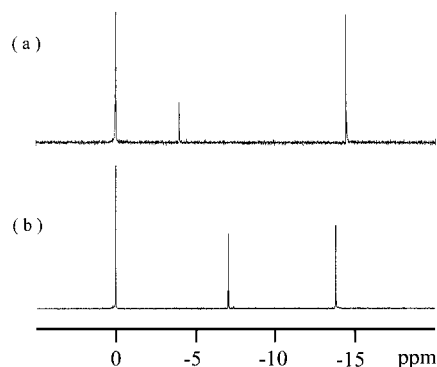


Figure 3. ^{31}P NMR spectra in D_2O of a) $\text{Na}_9[\mathbf{1a}] \cdot 16\text{H}_2\text{O}$ ($\mathbf{1}$) $\{\alpha\text{-}1,2,3\text{-P}_2\text{W}_{15}(\text{TiO}_2)_3\text{O}_{56}(\text{OH})_3\}^{9-}$ and b) $\text{Na}_x\text{H}_{33-x}[\mathbf{2a}] \cdot y\text{H}_2\text{O}$ ($\mathbf{2}$) ($x = 16\text{--}19$, $y = 60\text{--}70$; $\mathbf{2a} = \{\alpha\text{-}1,2,3\text{-P}_2\text{W}_{15}\text{Ti}_3\text{O}_{59}(\text{OH})_3\}_4[\mu_3\text{-Ti}(\text{OH})_3\text{Cl}]^{33-}$); the resonance at $\delta = 0.0$ ppm is due to the external reference 25% H_3PO_4 in H_2O ; in each case a very high level of purity is indicated (i.e., with respect to any other P-containing polyoxoanions or other materials)

Ti^{IV} -substituted Dawson POMs **2–4** listed in Table 1. Both the ^{183}W and ^{31}P NMR spectra are consistent with the solid-state structure.

Table 1. ^{31}P and ^{183}W NMR spectroscopic data of **1–4** in D_2O

Complex	δ (^{31}P NMR)	δ (^{183}W NMR)	Ref.
1	−3.93, −14.41	−156.5, −201.9, −230.1	this work
2	−7.04, −13.77	−145.0, −181.5, −201.4	[5a]
3	−7.6, −14.0	−148.3, −185.8, −211.2	[5b]
4	−7.3, −13.8		[5c]

Molecular Structure of **1a**

The crystal of **1** contains discrete cluster anions, sodium cations and lattice water molecules, all in general positions in the monoclinic space group $P2_1/c$. The solid-state packing of the polyoxoanions of **1a** is shown in Figure S2 in the Supporting Information. The observed electron densities of

the Ti and W atoms are quite different and the data unequivocally distinguish and define the Ti and W atoms. The 15 tungsten atoms, 3 titanium atoms and the 2 phosphorus atoms can be clearly identified. Thus, the main features of the molecular structure of the POM have been identified. However, the resolution obtained for the structure of the salt was limited by the poor quality of the available crystals and by the considerable disorder of the counteranions and the solvent of crystallization. Such a problem is common in POM crystallography.^[11]

The molecular structure of **1a** is composed of the monomeric Dawson POM unit “ $\alpha\text{-P}_2\text{W}_{15}\text{Ti}_3\text{O}_{62}$ ”, in which the

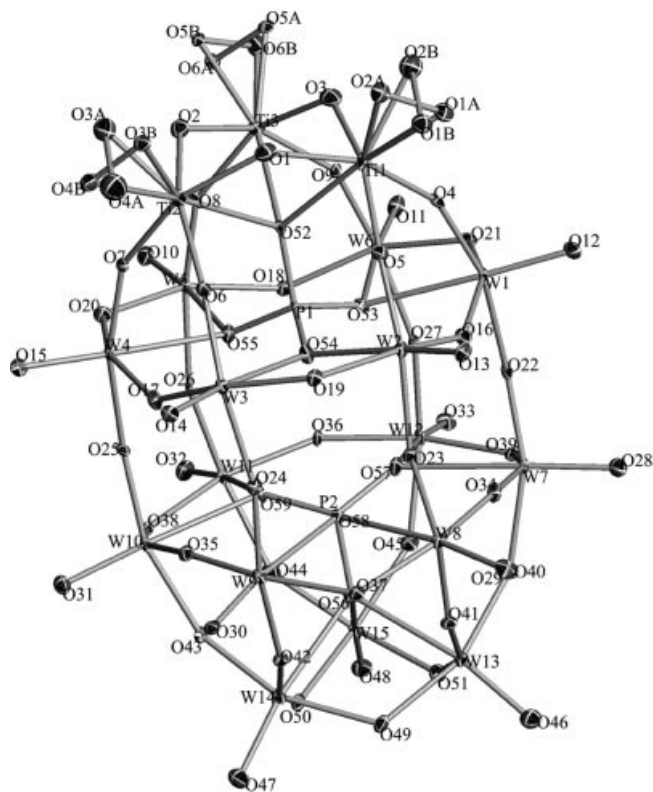
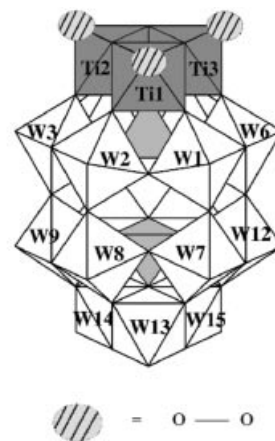


Figure 4. Top: polyhedral representation of the monomeric tris[peroxotitanium(IV)]-substituted Dawson POM $[\alpha\text{-}1,2,3\text{-P}_2\text{W}_{15}(\text{TiO}_2)_3\text{O}_{56}(\text{OH})_3]^{9-}$ (**1a**); bottom: molecular structure of **1a** with 50% probability ellipsoids

three edge-sharing octahedral sites of the titanium(IV) atoms (Ti_3 -cap site) in the " α - $\text{P}_2\text{W}_{15}\text{Ti}_3$ " Dawson unit substitute the three edge-sharing octahedral sites of the tungsten(VI) atoms (W_3 -cap site) of $[\alpha\text{-P}_2\text{W}_{18}\text{O}_{62}]^{6-}$. The 3 titanium atoms and 15 tungsten atoms in the Dawson unit all adopt conventional octahedral coordination polyhedra. The polyhedral representation and molecular structure of **1a** are shown in Figure 4 (top and bottom, respectively). In **1a**, the three terminal oxygen atoms of the Ti_3 cap are substituted by the side-on-coordinated peroxo groups (Figure 4, top). The peroxo groups coordinated to the titanium(IV) atoms are shown in two positions in Figure 4 (bottom) because of disorder. The site occupancy factors of the oxygen atoms in the peroxo group were fixed at 0.64 for those labelled A and 0.36 for those labelled B. Nevertheless, the three edge-sharing titanium(IV) octahedra were positively identified and have been more fully characterised, compared with the structures so far reported for other POM-based mono- and bis[peroxotitanium(IV)] complexes.^[3,4]

Selected bond lengths and angles around the three titanium(IV) centres and average bond lengths and angles for the Dawson POM unit in **1a** are given in Tables 2 and 3, respectively. The O–O distances of the peroxo groups [O1A–O2A 1.45(3), O3A–O4A 1.43(3), O5A–O6A 1.45(3) Å] indicate their single-bond nature.

The Ti–O distances in the Ti_3 cap (Ti1, Ti2, Ti3) are significantly influenced by the coordination of the peroxo group, whereas the W–O distances in the W_3 cap and the two W_6 belts, i.e. the W–Ot (Ot: terminal oxygen atom), W–Oe (Oe: edge-sharing oxygen atom), W–Oc (W belt) (Oc: corner-sharing oxygen atom) and W–Oa (Oa: oxygen atom coordinated to phosphorus atom) distances are in the normal ranges.^[1b] The Dawson unit contains two central P atoms in almost regular tetrahedral PO_4 units, i.e. the PO_4 closest to the Ti_3 cap [P–O distances 1.520(11)–1.560(11) Å; O–P–O angles 107.4(6)–110.9(6)°] and the PO_4 closer to the W_3 cap [P–O distances 1.513(12)–1.575(11) Å; O–P–O angles 106.8(6)–112.2(6)°].

Table 2. Selected bond lengths [Å] and angles [°] around the Ti_3 cap for **1a**

Ti–O–Ti distances		Ti–O–W distances			
Ti1–O1	2.001(13)	Ti1–O4	1.984(11)	W1–O4	1.806(13)
Ti2–O1	1.980(13)	Ti1–O5	1.963(11)	W2–O5	1.810(10)
Ti2–O2	1.975(12)	Ti2–O6	1.974(11)	W3–O6	1.813(11)
Ti3–O2	1.962(12)	Ti2–O7	1.991(11)	W4–O7	1.816(10)
Ti3–O3	1.986(13)	Ti3–O8	2.000(11)	W5–O8	1.806(11)
Ti1–O3	1.957(13)	Ti3–O9	1.982(11)	W6–O9	1.821(10)
Ti–Oa distances		Ti–O _{peroxo} distances			
Ti1–O52	2.360(11)	Ti1–O1A	1.84(2)	Ti2–O4A	1.88(2)
Ti2–O52	2.403(11)	Ti1–O2A	1.909(18)	Ti3–O5A	1.904(17)
Ti3–O52	2.372(11)	Ti2–O3A	1.92(2)	Ti3–O6A	1.894(17)
O–O distances					
O1A–O2A	1.45(3)	O3A–O4A	1.43(3)	O5A–O6A	1.45(3)
Angles					
Ti1–O1–Ti2	120.3(6)	Ti2–O7–W4	150.8(6)		
Ti2–O2–Ti3	123.0(6)	Ti3–O8–W5	151.5(7)		
Ti3–O3–Ti1	122.5(6)	Ti3–O9–W6	151.3(6)		
Ti1–O4–W1	152.3(6)	O1A–Ti1–O2A	45.5(8)		
Ti1–O5–W2	151.5(6)	O3A–Ti2–O4A	44.2(9)		
Ti2–O6–W3	152.7(6)	O5A–Ti3–O6A	44.8(8)		

Table 3. Average bond lengths [Å] and angles [°] for **1a**

	Cap W (13,14,15)	Cap Ti(1,2,3)
M–O(terminal)	1.707 (12) [1.705(12)–1.709(11)]	1.89(2) [1.84(2)–1.92(2)]
M–O(M cap)	1.937 (11) [1.918(11)–1.954(11)]	1.977(13) [1.957(13)–2.001(13)]
M–O(W belt)	1.870(11) [1.851(12)–1.890(11)]	1.982(11) [1.963(11)–2.000(11)]
M–O(P)	2.370(11) [2.352(11)–2.393(11)]	2.378(11) [2.360(11)–2.403(11)]
	Belt W(1–6)	Belt W(7–12)
W–O(terminal)	1.723(11) [1.698(12)–1.738(11)]	1.721(11) [1.706(12)–1.732(11)]
W–O(M cap)	1.812(11) [1.806(11)–1.821(10)]	1.985(11) [1.963(11)–2.002(10)]
W–O(W belt) ^[a]	1.921(11) [1.897(11)–1.952(11)]	1.914(11) [1.894(11)–1.929(11)]
W–O(W belt) ^[b]	1.899(11) [1.884(11)–1.917(11)]	1.891(11) [1.884(11)–1.904(11)]
W–O(W belt) ^[c]	2.002(10) [1.985(10)–2.031(10)]	1.822(10) [1.797(10)–1.834(10)]
W–O(P)	2.342(11) [2.322(11)–2.374(11)]	2.358(11) [2.323(10)–2.388(11)]
	W ₃ cap side	Ti ₃ cap side
P–O distance	1.537(11) [1.513(12)–1.575(11)]	1.541(11) [1.520(11)–1.560(11)]
O–P–O angle	109.4(6) [106.8(6)–112.2(6)]	109.5(6) [107.4(6)–110.9(6)]

^[a] Edge-sharing, between octahedra. ^[b] Corner-sharing, same belt. ^[c] Corner-sharing, between belts.

The calculated bond valence sums (BVS),^[12] based on observed bond lengths in **1a**, are in the range of 6.042–6.320 for the 15 tungsten atoms and 4.937–4.982 for the two phosphorus atoms. These data reasonably correspond to the formal valences of W^{6+} and P^{5+} , respectively. Furthermore, the BVS calculations of the oxygen atoms are in the range of 1.2322–1.2880 for O1, O2 and O3, indicating that a total of three protons are bound to the surface edge-sharing oxygen atoms of the Ti_3 cap in **1a**. In relation to this fact, we re-investigated the protonation sites and the actual anionic charges for **2a** and **3a** using BVS calculations and confirmed the protonation of all Ti–O–Ti bridges within the Dawson unit.^[6] Protonation of the μ_2 -oxo sites of the Ti–O–Ti bridges in the Dawson unit was first proposed for **4a**.^[5c] Thus, POM **1a** takes a total charge of -9 , suggesting that a peroxo group, but not a hydroperoxo group, is attached to each Ti atom.

The average O–O and Ti–O_{peroxo} bond lengths (1.44 and 1.89 Å, respectively) in **1a** can be compared with those of the previously reported mono[peroxotitanium(IV)] complex, OEP*Ti*(O₂) (OEP = 2,3,7,8,12,13,17,18-octaethylporphyrinato) which contains η^2 -coordination of the peroxo group to the titanium(IV) atom [O–O bond length 1.445(5) Å and two Ti–O distances 1.872(4) and 1.822(4) Å].^[10a] In comparison with other peroxo groups in the POM, the average O–O distance (1.44 Å) in **1a** is close to that in [α -P₂W₁₂(NbO₂)₆O₅₆]¹²⁻ (average 1.43 Å),^[13a] but shorter than that in [α,β -PW₉(NbO₂)O₃₇]⁶⁻ (average 1.51 Å)^[13b] and the noncoordinated O₂²⁻ group (average 1.49 Å).^[13c]

The peroxo groups influence the average bond lengths around the Ti_3 cap moiety more significantly than those around the W_3 cap moiety as evidenced by (i) the peroxo groups attached to the Ti atoms in **1a**, (ii) the intermolecular Ti–O–Ti interaction through the octahedral Ti^{IV} bridging groups in **2a** and (iii) the intermolecular Ti–O–Ti interaction due to direct linkage of the Dawson units in **3a** (Table 4). This effect would be reflected in the ³¹P and ¹⁸³W NMR resonances. In fact, the ³¹P resonance closest to the Ti_3 cap and the ¹⁸³W resonance of the W_6 belt closer to the Ti_3 cap are considerably more shifted (Table 1). Thus, the molecular structure of **1a** is consistent with the results of solution (³¹P and ¹⁸³W) NMR spectroscopy, suggesting that the tris[peroxotitanium(IV)] group containing Dawson structure is maintained in aqueous solution.

On standing at room temperature for a prolonged period of time (approximately a couple of weeks), an aqueous solution of **1a** formed new crystals. An X-ray structure analysis showed that the new crystals contain the tetrapod-shaped POM without the bridging octahedral Ti groups and without an encapsulated Cl⁻ ion, corresponding to the POM **4a** reported by Kortz et al.^[5c] In relation to this fact, two control experiments were performed as follows: (1) A clear orange solution of 0.3 g (0.067 mmol) of **1**, dissolved in 10 mL of water, was heated to reflux. ³¹P NMR spectra of the solution were measured after 1, 2, 12 and 19 h of heating at reflux. The orange colour of the solution remained for at least 3.5 h. After 12 h, the solution became colourless and a ³¹P NMR spectrum showed signals (δ = -7.40 and -14.16 ppm) due only to the giant tetrapod-POM without the bridging groups, i.e. **4a**. No ³¹P NMR signal for **1a** was observed. (2) The transformation of **1a** to **4a** was also confirmed by the reaction of **1a** (0.3 g, 0.067 mmol) with NaHSO₃ (0.5 g, 4.80 mmol) in aqueous solution at room temperature. Several minutes after mixing of **1a** with NaHSO₃, the solution became colourless. Compound **4a** had probably formed at this stage. After stirring overnight, the solution (which had been concentrated at 30 °C to about 2 mL) was added to 300 mL of EtOH and a white powder of **4**, showing ³¹P NMR resonances at δ = -7.31 and -14.05 ppm, was collected.

The transformation of **1a** to **4a** is due to thermal decomposition of the coordinated peroxo groups and also indicates the potential of **1a** as a nanobuilding block for formation of POM-based giant molecules. The peroxo group attached to the Ti atoms was relatively stable and the catalytic activity of **1a** for 2-propanol oxidation with aqueous H₂O₂ was very low. Thus, POM **1a** can be expected to act as a building block for the preparation of POM-based giant molecules, rather than as an oxidation catalyst. It is likely that the catalytically active species will be the hydroperoxotitanium(IV) species rather than the peroxotitanium(IV) species.^[3c]

Conclusion

In conclusion, the monomeric tris[peroxotitanium(IV)]-substituted α -Dawson POM [α -1,2,3-P₂W₁₅(TiO₂)₃O₅₆-

Table 4. Comparison of average bond lengths [Å] [range] around the Ti_3 caps for Dawson POM units in **1a**–**3a**

	1a	2a ^[a]
Ti–O(terminal)	1.89(2) [1.84(2)–1.92(2)]	1.78(2) [1.77(2)–1.79(2)]
Ti–O(Ti cap)	1.977(13) [1.957(13)–2.001(13)]	2.01(2) [1.98(2)–2.05(2)]
Ti–O(W belt)	1.982(11) [1.963(11)–2.000(11)]	1.89(2) [1.87(2)–1.94(2)]
Ti–O(P)	2.378(11) [2.360(11)–2.403(11)]	2.29(2) [2.27(2)–2.30(2)]
	3a ^[b]	
Ti–O(terminal)	1.823(15) [1.809(15)–1.845(15)]	
Ti–O(Ti cap)	1.934(15) [1.888(15)–1.955(14)]	
Ti–O(W belt)	1.959(15) [1.937(15)–1.982(16)]	
Ti–O(P)	2.267(14) [2.242(15)–2.307(14)]	

[a] Ref.^[5a] [b] Ref.^[5b].

(OH)₃]⁹⁻ (**1a**), showing η^2 -coordination of the peroxo group, was obtained from the reaction of an excess of 30% aqueous H₂O₂ with the recently reported giant tetrapod-shaped POM { $[\alpha$ -1,2,3-P₂W₁₅Ti₃O₅₉(OH)₃]₄[μ_3 -Ti(OH)₃]₄Cl}³³⁻ (**2a**) (FW \approx 16000) with approximately T_d symmetry. The water-soluble compound isolated as Na₉[**1a**] \cdot 16H₂O (**1**) can be expected to be suitable as a precursor for the synthesis of novel POM-based giant molecules.

Experimental Section

Materials: The following were used as received: Na₂WO₄ \cdot 2H₂O, 85% H₃PO₄, KCl, NaCl, NaClO₄, 12 M aqueous HCl solution (quantitative analysis grade), 30% aqueous H₂O₂ solution, TiCl₄ (all from Wako) and D₂O (Isotec). The synthesis and characterisation of the tetrameric precursor **2** have been reported elsewhere.^[5a]

Instrumentation/Analytical Procedure: A complete elemental analysis was carried out by Mikroanalytisches Labor Pascher (Remagen, Germany). The sample was dried at room temperature at 10^{-3} – 10^{-4} Torr overnight before analysis. IR spectra were recorded with a Jasco 300 FT-IR spectrometer in KBr disks at room temperature. Thermogravimetric (TG) and differential thermal analyses (DTA) were acquired with a Rigaku TG8101D and TAS 300 data processing system. TG/DTA measurements were carried out in air with a temperature ramp of 4 °C per min between 25 and 500 °C. ³¹P NMR (161.70 MHz) spectra in D₂O were recorded in 5-mm outer-diameter tubes with a JEOL JNM-EX 400 FT NMR spectrometer and a JEOL EX-400 NMR spectroscopic data-processing system. ³¹P NMR spectra were referenced to an external standard of 25% H₃PO₄ in H₂O in a sealed capillary. Chemical shifts were reported on the δ scale with resonances upfield of H₃PO₄ (δ = 0 ppm) as negative. ¹⁸³W NMR (16.50 MHz) spectra were recorded in 10-mm outer-diameter tubes with a JEOL JNM-EX 400 FT NMR spectrometer equipped with a JEOL NM-40T10 L low-frequency tuneable probe and a JEOL EX-400 NMR spectroscopic data-processing system. ¹⁸³W NMR spectra measured in D₂O were referenced to an external standard of saturated Na₂WO₄ in D₂O (δ = 0 ppm). Chemical shifts were reported as negative for resonances upfield of Na₂WO₄ (δ = 0 ppm).

Synthesis of **1 as a Powder:** To a stirred, clear, colourless solution of the precursor **2**^[5a,6] (2.1 g, ca. 0.12 mmol), dissolved in water (16 mL), was added 30% aq. H₂O₂ (1.0 mL, 12.7 mmol). The clear red solution was stirred for 1 h and NaCl (5.0 g, 86.0 mmol) was then added. After stirring for 1 h, a red-orange powder formed which was collected on a membrane filter (JG 0.2 μ m), washed with ethanol (10 mL \times 2) and diethyl ether (50 mL \times 2). The crude product at this stage was obtained in a quantity of about 1.0 g. The yellow-orange powder was dissolved in water (10 mL). The clear red-orange solution was concentrated to ca. 3 mL using a rotary evaporator at 35 °C and the resultant solution was placed in a refrigerator at 5 °C. After 1 d, the orange crystalline compound **1** was collected on a membrane filter (JG 0.2 μ m), washed with ethanol (10 mL \times 2) and diethyl ether (50 mL \times 2) and dried in vacuo for 2 h. A yellow-orange powder of **1** was obtained in ca. 25% (0.53 g) yield. Compound **1** is highly soluble in water but insoluble in diethyl ether and ethanol. Na₉[P₂W₁₅(TiO₂)₃O₅₆(OH)₃] \cdot 4H₂O = H₁₁Na₉O₆₉P₂Ti₃W₁₅ (4285.29): calcd. H 0.26, Na 4.83, O 25.76, P 1.45, Ti 3.35, W 64.35; found H 0.38, Na 4.61, O 25.5, P 1.40, Ti 3.36, W 63.5, Cl < 0.03; total 98.85%. A weight loss of 4.93%

was observed during the course of drying at room temperature at 10^{-3} – 10^{-4} Torr overnight before the elemental analysis. This suggests the presence of 12–13 water molecules weakly or adsorbed. Using TG/DTA under atmospheric conditions, a weight loss of 6.61% was observed below 167.4 °C with endothermic points at 60.2 and 83.9 °C; calcd. 6.44% for x = 16 in Na₉[P₂W₁₅(TiO₂)₃O₅₆(OH)₃] \cdot x H₂O. A weight loss of 4.12% observed from 167 °C up to ca. 400 °C with an endothermic point at 172 °C is due to decomposition of the coordinated peroxo groups. IR (KBr) (polyoxometalates region): $\tilde{\nu}$ = 1083 s, 1054 m, 1013 w, 1002 w, 940 vs, 923 vs, 891 s, 820 vs, br, 811 vs, br, 755 m, 707 m, 612 m, 599 m, 559 m, 527 m, 487 w, 465 w, 431 w cm⁻¹. ³¹P NMR (21.3 °C, D₂O): δ = -3.93, -14.41 ppm. ¹⁸³W NMR (20.7 °C, D₂O): δ = -156.5 (3 W), -201.9 (6 W), -230.1 (6 W) ppm.

Crystallisation of **1:** Compound **1** (1.89 g) was dissolved in water (20 mL) and filtered through a folded filter paper (Whatman No. 2). The clear orange filtrate was concentrated to ca. 3 mL using a rotary evaporator at 30 °C. The solution was divided into two portions and slow concentration of both at room temperature was allowed to occur. After 3 d, clear orange plate crystals formed. One portion was used for X-ray diffraction measurements and the other for characterisation purposes. The crystals of one portion (1.5 mL) amounted to 0.17 g (8.99% yield). The characterisation data of the crystals using TG/DTA, IR and ³¹P NMR spectroscopy are in agreement with those of the powder sample, suggesting that the crystals were representative of the bulk sample.

X-ray Crystallography for **1:** A clear orange plate crystal of **1** (0.26 \times 0.16 \times 0.06 mm) was picked up with a cryo loopTM (from Hampton Research) and coated with liquid paraffin to prevent its degradation. Data were collected with a Bruker SMART APEX CCD diffractometer at 90 K in the range $1.8^\circ < 2\theta < 56.7^\circ$. The intensity data were automatically corrected for Lorentz and polarisation effects during integration. The structure was solved by direct methods (SHELXS-97: G. M. Sheldrick, University of Göttingen, 1990) followed by subsequent difference Fourier calculations and refined by full-matrix least-squares procedures (SHELXS-97: G. M. Sheldrick, University of Göttingen, 1997). The site occupancy factors of the oxygen atoms in the peroxo group were fixed at 0.64 for those labelled A and 0.36 for those labelled B. Crystal data for H₃₅Na₉O₈₁P₂Ti₃W₁₅, M = 4501.58, monoclinic, space group $P2_1/c$ (no. 14), a = 23.118(3), b = 15.2478(19), c = 24.967(3) Å, β = 100.247(2)°, V = 8660.4(19) Å³, Z = 4, $\rho_{\text{calcd.}}$ = 3.453 g cm⁻³, $\mu(\text{Mo-K}\alpha)$ = 20.28 mm⁻¹, R_{int} = 0.1912, $R1$ = 0.0643, $wR2$ = 0.1904, GOF = 1.054 [103259 total reflections, 21557 unique reflections were $I > 2\sigma(I)$] [$R1$ = 0.0845, $wR2$ = 0.2025 (for all data)]. The maximum and minimum residual densities (10.29 and -4.784, respectively) were located at 2.31 Å from O29 and 1.11 Å from W3, respectively. In the X-ray crystallography of **1** there are several points to be addressed. (1) Absorption correction: the product of μ and t_{mid} is greater than 3. Since an oil was used for the diffraction measurements, numerical correction of the absorption is actually impossible. (2) In the structure analysis, disorder treatment was used. There are some short O–O distances (less than 1.5 Å), that is, distances between water molecules. This is necessary because the occupancy of O was set at less than 0.5. The positions of the hydrogen atoms of the water molecule could not be determined. (3) The larger residual electron density peaks still remain and a greater R_{int} (> 0.15) results. It is actually impossible to obtain high-quality diffraction data from the POM because of the disorder of the solvent in the crystal and the difficulties applying absorption corrections. Further details on the crystal structure investigation may be obtained from the Fachinformationzen-

trum Karlsruhe, 76344 Eggenstein-Leopoldshafen, Germany [Fax: (internat.) + 49-7247-808-666; E-mail: crysdata@fiz-karlsruhe.de], on quoting the depository number CSD-413816 (formula/code: yos20mo).

Reactivity of 2a and 3a with Aqueous Hydrogen Peroxide: The reaction of the giant tetrapod-shaped POM **2a** with hydrogen peroxide gave a pure form of the peroxo species **1a** within 30 min. In contrast, the reaction of another giant tetrapod-shaped POM (**3a**) with hydrogen peroxide, which was monitored by ^{31}P NMR spectroscopy, did not react in the same way. To a colourless solution of **3** (0.52 g, 0.029 mmol), dissolved in water (5 mL), was added 30% aqueous H_2O_2 (0.25 mL, 3.18 mmol). The colour of the solution became clear yellow after 30 min, yellow-orange after 9 h and orange after 35 h. A ^{31}P NMR spectrum of the solution, measured after 30 min, showed only a two-line spectrum with resonances $\delta = -7.70$ and -13.97 ppm due to **3a** itself, indicating that no peroxo species was formed. After 9 h, the two ^{31}P NMR signals at $\delta = -4.24$ and -14.16 ppm, assignable to the peroxo species **1a**, began to appear but the large signals (at $\delta = -7.70$, -13.97 ppm) of **3a** still remained and smaller peaks due to at least three other species (at $\delta = -5.18$, -5.38 , -6.90 and -14.23 ppm) could also be observed. After 35 h, the ^{31}P NMR signals due to the peroxo species **1a** at $\delta = -4.15$ and -14.06 ppm, as well as other peaks due to at least three species (at $\delta = -5.09$, -5.30 , -6.80 , -13.81 , -14.14 ppm), became larger, whereas only the two signals due to **3a** (at $\delta = -7.62$ and -13.88 ppm) became less intense. After a prolonged reaction time of **3a**, the formation of the peroxo species **1a** was definitely confirmed. However, **1a** was not the only species formed. Thus, with hydrogen peroxide, the reactivity of compound **3a** was quite different from that of **2a**.

Supporting Information: Figures S1 and S2; see also the footnote on the first page of this article

Acknowledgments

This work was supported by a Grant-in-Aid for Scientific Research and also by a High-tech Research Centre Project, both from the Ministry of Education, Culture, Sports, Science and Technology, Japan. We thank Akira Shinohara for evaluation of the catalytic activity of **1a** for 2-propanol oxidation with 30% aqueous hydrogen peroxide.

- [1] [1a] M. T. Pope, A. Müller, *Angew. Chem. Int. Ed. Engl.* **1991**, *30*, 34. [1b] M. T. Pope, *Heteropoly and Isopoly Oxometalates*, Springer-Verlag, New York, **1983**. [1c] V. W. Day, W. G. Klempner, *Chem. Rev.* **1985**, *228*, 533. [1d] C. L. Hill, *Chem. Rev.* **1998**, *98*, 1. [1e] T. Okuhara, N. Mizuno, M. Misono, *Adv. Catal.* **1996**, *41*, 113. [1f] C. L. Hill, C. M. Prosser-McCarthy, *Coord. Chem. Rev.* **1995**, *143*, 407. [1g] A series of 34 recent papers in a volume devoted to poloxoanion in catalysis: C. L. Hill, *J. Mol. Catal.* **1996**, *114*, 1. [1h] R. Neumann, *Prog. Inorg. Chem.* **1998**, *47*, 317. [1i] *Polyoxometalate Chemistry from Topology via Self-Assembly to Applications* (Eds: M. T. Pope, A. Müller), Kluwer Academic Publishers, Netherlands, **2001**. [1j] *Polyoxometalate Chemistry for Nano-Composite Design* (Eds: T. Yamase, M. T. Pope), Kluwer Academic Publishers, Netherlands, **2002**. [1k] M. T. Pope, "Polyoxo anions: synthesis and structure", in *Comprehensive Coordination Chemistry II* (Ed.: A. G. Wedd), Elsevier Science, New York, **2004**, vol. 4, p. 635.
- [2] [2a] U. Müller, *Inorganic Structural Chemistry*, Wiley, New York, **1993**. [2b] A. L. Linsenbiger, G. Lu, J. T. Yates, Jr., *Chem. Rev.*

- 1995**, *95*, 735. [2c] T. Kawahara, Y. Konishi, H. Tada, N. Tohge, J. Nishii, S. Ito, *Angew. Chem. Int. Ed.* **2002**, *41*, 2811.
- [3] [3a] F. Gao, T. Yamase, H. Suzuki, *J. Mol. Catal. A: Chem.* **2002**, *180*, 97. [3b] T. Yamase, E. Ishikawa, Y. Asai, S. Kanai, *J. Mol. Catal. A: Chem.* **1996**, *114*, 237. [3c] O. A. Kholdeeva, G. M. Maksimov, R. I. Maksimovskaya, L. A. Kovaleva, M. A. Fedotov, V. A. Grigoriev, C. L. Hill, *Inorg. Chem.* **2000**, *39*, 3828.
- [4] T. Yamase, T. Ozeki, S. Motomura, *Bull. Chem. Soc. Jpn.* **1992**, *65*, 1453.
- [5] [5a] Y. Sakai, K. Yoza, C. N. Kato, K. Nomiya, *Chem. Eur. J.* **2003**, *9*, 4077. [5b] Y. Sakai, K. Yoza, C. N. Kato, K. Nomiya, *Dalton Trans.* **2003**, 3581. [5c] U. Kortz, S. S. Hamzeh, A. Nasser, *Chem. Eur. J.* **2003**, *9*, 2945. [5d] K. Nomiya, Y. Arai, Y. Shimizu, M. Takahashi, T. Takayama, H. Weiner, T. Nagata, J. A. Widegren, R. G. Finke, *Inorg. Chim. Acta* **2000**, *300–302*, 285.
- [6] Abbreviation of compounds **1–4**: Previous formulae of **2** and **2a**^[5a] as well as **3** and **3a**^[5b] were revised by considering the protonation sites in the Dawson unit found with BVS calculations of the oxygen atoms; (1) tris[peroxotitanium(IV)]-substituted Dawson POM $\text{Na}_3[\mathbf{1a}] \cdot 16\text{H}_2\text{O}$ (**1**) {**1a** = $[\alpha\text{-}1,2,3\text{-P}_2\text{W}_{15}(\text{TiO}_2)_3\text{O}_{56}(\text{OH})_3]^{9-}$ }, (2) giant tetrapod-POM with the bridging Ti octahedral groups $\text{Na}_x\text{H}_{33-x}[\mathbf{2a}] \cdot y\text{H}_2\text{O}$ (**2**) ($x = 16\text{--}19$, $y = 60\text{--}70$; **2a** = $\{[\alpha\text{-}1,2,3\text{-P}_2\text{W}_{15}\text{Ti}_3\text{O}_{59}(\text{OH})_3]_4[\mu_3\text{-Ti}(\text{OH})_3]_4\text{Cl}\}^{33-}$), (3) giant tetrapod-POM without the bridging groups $\text{K}_4\text{Na}_{21}[\mathbf{3a}] \cdot y\text{H}_2\text{O}$ (**3**) ($y = 60\text{--}70$; **3a** = $\{[\alpha\text{-}1,2,3\text{-P}_2\text{W}_{15}\text{Ti}_3\text{O}_{57.5}(\text{OH})_3]_4\text{Cl}\}^{25-}$), and (4) giant tetrapod-POM without the bridging groups and without the encapsulated Cl^- ion $\text{K}_4(\text{NH}_4)_{20}[\mathbf{4a}] \cdot 77\text{H}_2\text{O}$ (**4**) {**4a** = $[\text{P}_2\text{W}_{15}\text{Ti}_3\text{O}_{57.5}(\text{OH})_3]_4^{24-}$ }. [5c]
- [7] At present, we can consider at least four giant tetrapod-shaped POMs with regard to the presence of the bridging Ti octahedral groups and/or the presence of an encapsulated chloride ion. Three of them (**2a**, **3a** and **4a**) have been confirmed.^[5a–5c] The encapsulated chloride ion in **3a** can be removed from the POM by recrystallisation from an aqueous solution containing KCl and HCl.^[5d]
- [8] Formation conditions of the two tetrameric Dawson POMs **2a** and **3a** were examined by ^{31}P NMR measurements in aqueous solution (Figure S1, see Supporting Information, see also the footnote on the first page of this article). One key for their formation is the concentration of the titanium(IV) ion used in the reaction. POM **3a** was formed in solution at a 3:1 molar ratio of $\text{Ti}(\text{SO}_4)_2 \cdot 4\text{H}_2\text{O} / \text{Na}_{12}[\text{B-}\alpha\text{-P}_2\text{W}_{15}\text{O}_{56}] \cdot 19\text{H}_2\text{O}$, while POM **2a** was formed in solution at a 10:1 molar ratio.
- [9] C. Rocchiccioli-Deltcheff, R. Thouvenot, *Spectrosc. Lett.* **1979**, *12*, 127.
- [10] [10a] R. Guillard, J.-M. Latour, C. Lecomte, J.-C. Marchon, J. Protas, D. Ripoll, *Inorg. Chem.* **1978**, *17*, 1228. [10b] P. E. Esser, U. Englert, W. Keim, *Chem. Ber.* **1996**, *129*, 833.
- [11] [11a] T. J. R. Weakley, R. G. Finke, *Inorg. Chem.* **1990**, *29*, 1235. [11b] Y. Lin, T. J. R. Weakley, B. Rapko, R. G. Finke, *Inorg. Chem.* **1993**, *32*, 5095. [11c] T. Yamase, T. Ozeki, H. Sakamoto, S. Nishiyama, A. Yamamoto, *Bull. Chem. Soc. Jpn.* **1993**, *66*, 103. [11d] K. Nomiya, M. Takahashi, K. Ohsawa, J. A. Widegren, *J. Chem. Soc., Dalton Trans.* **2001**, 2872. [11e] K. Nomiya, M. Takahashi, J. A. Widegren, T. Aizawa, Y. Sakai, N. C. Kasuga, *J. Chem. Soc., Dalton Trans.* **2002**, 3679.
- [12] [12a] I. D. Brown, D. Altermatt, *Acta Crystallogr., Sect. B* **1985**, *41*, 244. [12b] I. D. Brown, R. D. Shannon, *Acta Crystallogr., Sect. A* **1973**, *29*, 266.
- [13] [13a] D. A. Judd, Q. Chen, C. F. Campana, C. L. Hill, *J. Am. Chem. Soc.* **1997**, *119*, 5461. [13b] M. K. Harrup, G.-S. Kim, H. Zeng, R. P. Johnson, D. VanDerveer, C. L. Hill, *Inorg. Chem.* **1998**, *37*, 5550. [13c] L. Vaska, *Acc. Chem. Res.* **1976**, *9*, 175.

Received July 19, 2004

Early View Article

Published Online October 18, 2004